

# Soft-gluon corrections for single top quark production in association with electroweak bosons

MATTHEW FORSLUND\* AND NIKOLAOS KIDONAKIS

*Department of Physics, Kennesaw State University,  
Kennesaw, GA 30144, USA*

**Abstract:** We present results for higher-order soft-gluon radiative corrections for single top-quark production in association with electroweak bosons, including  $t\gamma$  and  $tZ$  production via anomalous FCNC couplings. We provide results for the total cross sections and differential distributions at LHC energies. We use  $K$ -factors to show the significance of the corrections compared to leading order, and we discuss uncertainties and the importance of the results.

*\*Talk presented at the 2019 Meeting of the Division of Particles and Fields of the American Physical Society (DPF2019), July 29–August 2, 2019, Northeastern University, Boston, C1907293.*

## 1 Introduction

Top-quark production at the Large Hadron Collider (LHC) remains an active area of searches for physics beyond the Standard Model, including searches for anomalous couplings [1–3]. In some new physics models, top quarks can be produced via processes involving flavor-changing neutral currents (FCNC). Two such processes are the production of  $t\gamma$  [4–11] and  $tZ$  [4,5,8–10,12,13] pairs without additional quarks in the final state.

The effective Lagrangian involving anomalous FCNC couplings of a  $tq$  pair to electroweak bosons, with  $q$  an up or charm quark, is given by

$$\Delta\mathcal{L}^{eff} = \frac{1}{\Lambda} \kappa_{tqA} e \bar{t} \sigma_{\mu\nu} q F_A^{\mu\nu} + h.c., \quad (1)$$

where  $\kappa_{tqA}$  is the anomalous coupling, with  $A$  a photon or  $Z$ -boson,  $\Lambda$  is an effective scale which is taken to be the top-quark mass,  $F_A^{\mu\nu}$  are the appropriate electroweak-boson field tensors, and  $\sigma_{\mu\nu} = (i/2)(\gamma_\mu\gamma_\nu - \gamma_\nu\gamma_\mu)$  where  $\gamma_\mu$  are the Dirac matrices.

To improve experimental limits on these anomalous FCNC couplings, it is important to have a good theoretical prediction, which entails studying higher-order corrections. We calculate higher-order corrections to  $gq \rightarrow tZ$  and  $gq \rightarrow t\gamma$  arising from soft-gluon radiation. These soft-gluon corrections enhance the leading-order (LO) cross sections, and they dominate (and thus approximate well) the higher-order corrections. The approximate next-to-leading order (aNLO) and approximate next-to-next-to-leading order (aNNLO) corrections from soft-gluon emission were studied for the processes  $gq \rightarrow tZ$  and  $gq \rightarrow t\gamma$  in [14] and [15], respectively. We present detailed results for cross sections and differential distributions for both processes at LHC energies through aNNLO, and also some approximate next-to-next-to-next-to-leading order (aNNNLO) results. More details on soft-gluon resummation and top-quark production can be found in the review in Ref. [16].

## 2 Soft-gluon corrections

For the partonic process  $g(p_g) + q(p_q) \rightarrow t(p_t) + A(p_A)$ , where  $A$  represents a  $Z$ -boson or a photon, we define the kinematical variables  $s = (p_g + p_q)^2$ ,  $t = (p_g - p_t)^2$ ,  $u = (p_q - p_t)^2$ , and  $s_4 =$

$s + t + u - m_t^2 - m_A^2$ , where  $m_A = m_Z$  for the  $Z$ -boson mass and  $m_A = m_\gamma = 0$  for the photon, and  $m_t$  is the top-quark mass. Near partonic threshold, i.e. when there is just enough energy to produce the final  $tA$  state, but with the top quark and electroweak boson not necessarily at rest, we have  $s_4 \rightarrow 0$ . We also define  $t_1 = t - m_t^2$ ,  $t_2 = t - m_A^2$ ,  $u_1 = u - m_t^2$ , and  $u_2 = u - m_A^2$ .

We consider the double-differential partonic cross section  $d^2\hat{\sigma}_{gq \rightarrow tA}^{(n)}/(dt du)$  at  $n$ th order. The LO cross section is

$$\frac{d^2\hat{\sigma}_{gq \rightarrow tA}^{(0)}}{dt du} = F_{gq \rightarrow tA}^{\text{LO}} \delta(s_4), \quad (2)$$

where

$$\begin{aligned} F_{gq \rightarrow tA}^{\text{LO}} &= \frac{e^2 \alpha_s \kappa_{tqA}^2}{6s^3 t_1^2} \left\{ 2m_t^6 - m_t^4(3m_A^2 + 4s + 2t) + m_t^2 [2m_A^4 - m_A^2(2s + t) + 2(s^2 + 4st + t^2)] \right. \\ &\quad + 2m_A^6 - 4m_A^4 t + m_A^2(s + t)(s + 5t) - 2t(3s^2 + 6st + t^2) \\ &\quad \left. - \frac{t}{m_t^2} [2m_A^6 - 2m_A^4(s + t) + m_A^2(s + t)^2 - 4st(s + t)] \right\}, \end{aligned} \quad (3)$$

with  $\alpha_s$  the strong coupling.

The structure of the soft-gluon corrections is governed by a soft anomalous dimension,  $\Gamma^S$ . For next-to-leading-logarithm (NLL) accuracy, we need one-loop results. The one-loop expression for the soft anomalous dimension in Feynman gauge is given by

$$\Gamma_{gq \rightarrow tA}^{S(1)} = C_F \left[ \ln \left( \frac{-u_1}{m\sqrt{s}} \right) - \frac{1}{2} \right] + \frac{C_A}{2} \ln \left( \frac{t_1}{u_1} \right) \quad (4)$$

where  $C_F = (N_c^2 - 1)/(2N_c)$  and  $C_A = N_c$ , with  $N_c = 3$  the number of colors. Two-loop [14, 15] and three-loop [17] expressions are also available but they are not required for the NLL accuracy that we use here.

The aNLO soft-gluon corrections for  $gq \rightarrow tA$  are

$$\frac{d^2\hat{\sigma}_{gq \rightarrow tA}^{(1)}}{dt du} = F_{gq \rightarrow tA}^{\text{LO}} \frac{\alpha_s(\mu_R^2)}{\pi} \left\{ c_3 \left[ \frac{\ln(s_4/m_t^2)}{s_4} \right]_+ + c_2 \left[ \frac{1}{s_4} \right]_+ + c_1 \delta(s_4) \right\}, \quad (5)$$

where  $c_3 = 2(C_F + C_A)$ ,

$$c_2 = 2C_F \ln \left( \frac{u_1}{t_2} \right) - C_F + C_A \ln \left( \frac{t_1}{u_1} \right) + C_A \ln \left( \frac{sm_t^2}{u_2^2} \right) - (C_F + C_A) \ln \left( \frac{\mu_F^2}{m_t^2} \right), \quad (6)$$

$$c_1 = \left[ C_F \ln \left( \frac{-t_2}{m_t^2} \right) + C_A \ln \left( \frac{-u_2}{m_t^2} \right) - \frac{3}{4} C_F \right] \ln \left( \frac{\mu_F^2}{m_t^2} \right) - \frac{\beta_0}{4} \ln \left( \frac{\mu_F^2}{\mu_R^2} \right), \quad (7)$$

$\mu_F$  is the factorization scale,  $\mu_R$  is the renormalization scale, and  $\beta_0 = (11C_A - 2n_f)/3$  is the lowest-order QCD  $\beta$  function, with  $n_f = 5$  the number of light-quark flavors.

The aNNLO soft-gluon corrections for  $gq \rightarrow tA$  are

$$\begin{aligned} \frac{d^2\hat{\sigma}_{gq \rightarrow tA}^{(2)}}{dt du} &= F_{gq \rightarrow tA}^{\text{LO}} \frac{\alpha_s^2(\mu_R^2)}{\pi^2} \left\{ \frac{1}{2} c_3^2 \left[ \frac{\ln^3(s_4/m_t^2)}{s_4} \right]_+ + \left[ \frac{3}{2} c_3 c_2 - \frac{\beta_0}{4} c_3 \right] \left[ \frac{\ln^2(s_4/m_t^2)}{s_4} \right]_+ \right. \\ &\quad + \left[ c_3 c_1 - (C_F + C_A)^2 \ln^2 \left( \frac{\mu_F^2}{m_t^2} \right) - 2(C_F + C_A) c_2 \ln \left( \frac{\mu_F^2}{m_t^2} \right) + \frac{\beta_0}{4} c_3 \ln \left( \frac{\mu_R^2}{m_t^2} \right) \right] \left[ \frac{\ln(s_4/m_t^2)}{s_4} \right]_+ \\ &\quad \left. + (C_F + C_A) \left[ -c_1 \ln \left( \frac{\mu_F^2}{m_t^2} \right) - \frac{\beta_0}{4} \ln \left( \frac{\mu_F^2}{m_t^2} \right) \ln \left( \frac{\mu_R^2}{m_t^2} \right) + \frac{\beta_0}{8} \ln^2 \left( \frac{\mu_F^2}{m_t^2} \right) \right] \left[ \frac{1}{s_4} \right]_+ \right\}. \end{aligned} \quad (8)$$

### 3 $gu \rightarrow tZ$ via anomalous top-quark couplings

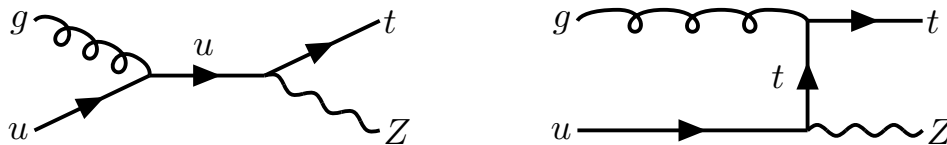


Figure 1: Tree-level diagrams for  $tZ$  production via anomalous couplings.

We first present results for  $gu \rightarrow tZ$  production. The LO Feynman diagrams contributing to the process are shown in Fig. 1. Numerical results for the total cross section are given in Fig. 2. We use MMHT2014 [18] NNLO parton distribution functions (PDFs) and take  $\kappa_{tqZ} = 0.01$ . The results in [14] use CT14 [19] PDFs; however, those results are very similar to the ones presented here. The left plot shows the total aNNLO cross section as a function of top quark mass at LHC energies of 7, 8, 13, and 14 TeV, with  $K$ -factors relative to aNLO shown in the inset. We show a more detailed breakdown at 13 TeV LHC energy in the right plot, showing LO, aNLO, aNNLO, and aNNNLO cross sections, as well as  $K$ -factors over LO in the inset. We find that the increase in the cross section is substantial at aNNLO for all energies in the plots, with a 49% increase in the total cross section at 13 TeV at aNNLO compared to the 36% increase at aNLO. The further contribution from aNNNLO corrections is much smaller.

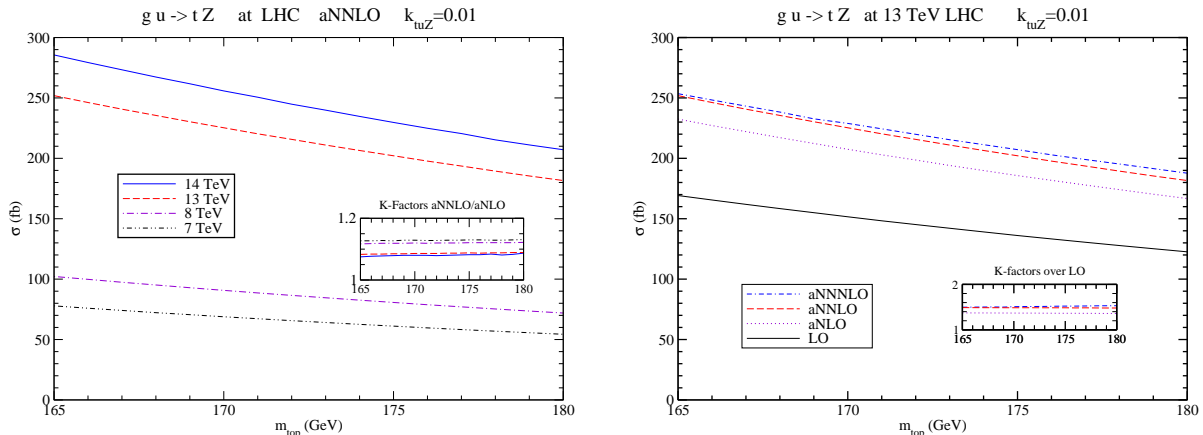


Figure 2: The left plot shows results for the total aNNLO cross section for  $gu \rightarrow tZ$  at 7, 8, 13, and 14 TeV as a function of top-quark mass. Its inset shows aNNLO/aNLO  $K$ -factors. The right plot shows the total LO, aNLO, aNNLO, and aNNNLO cross section at 13 TeV as a function of top-quark mass. Its inset shows  $K$ -factors relative to LO.

Differential distributions in top-quark rapidity and transverse momentum are shown in Fig. 3, where we see a similarly significant impact by the higher-order corrections. For more details on the soft-gluon corrections to  $gq \rightarrow tZ$  and further numerical results, including results for charm-quark initial states and scale dependence, see Ref. [14].

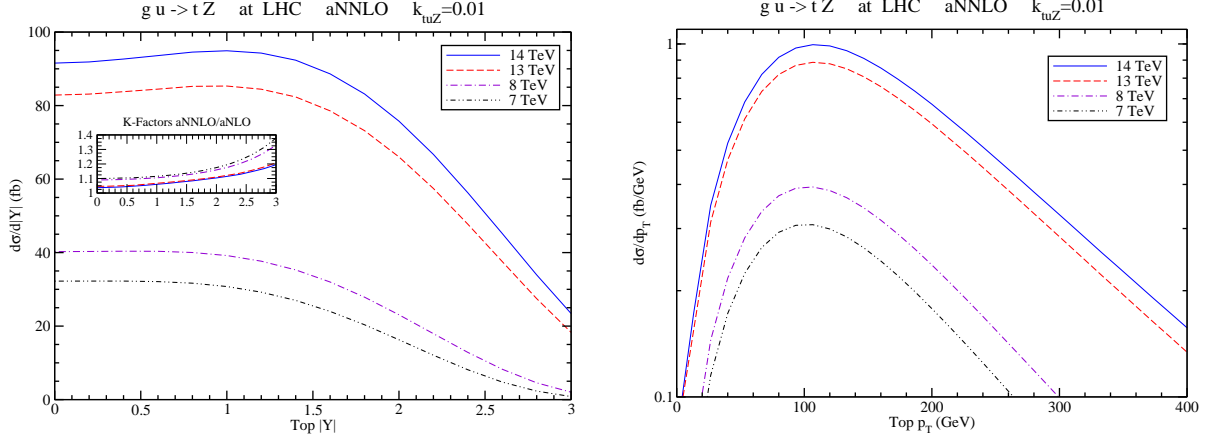


Figure 3: Differential aNNLO rapidity (left plot) and transverse-momentum (right plot) distributions for  $gu \rightarrow tZ$  at LHC energies of 7, 8, 13, and 14 TeV. The inset of the rapidity plot also includes  $K$ -factors over aNLO.

#### 4 $gu \rightarrow t\gamma$ via anomalous top-quark couplings

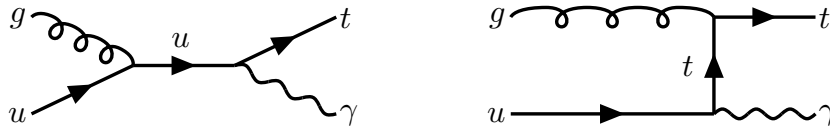


Figure 4: Tree-level diagrams for  $t\gamma$  production via anomalous couplings.

We continue with results for  $gu \rightarrow t\gamma$ . The LO Feynman diagrams describing the process are shown in Fig. 4, and are analogous to those for  $gu \rightarrow tZ$ . Just as with the process  $gu \rightarrow tZ$ , we use MMHT2014 [18] NNLO PDFs and take  $\kappa_{t\gamma} = 0.01$ . The left plot shows results for the total aNNLO cross section as a function of top-quark mass at LHC energies of 7, 8, 13, and 14 TeV, with  $K$ -factors relative to aNLO shown in the inset. The right plot shows a more detailed breakdown at 13 TeV of the total cross section at LO, aNLO, aNNLO, and aNNNLO, with  $K$ -factors over LO shown in the inset. Similarly to  $gu \rightarrow tZ$ , we find a significant increase in the cross section at aNLO and aNNLO, with much smaller contributions from aNNNLO. At 13 TeV, the NLO corrections provide a 31% increase in the cross section, and the aNNLO results provide a 36% increase. The differential distributions shown in Fig. 6 experience a similarly significant increase by the higher-order corrections. For more details on the soft-gluon corrections to  $gq \rightarrow t\gamma$  and further numerical results, including scale dependence and results for charm-quark initial states, see Ref. [15].

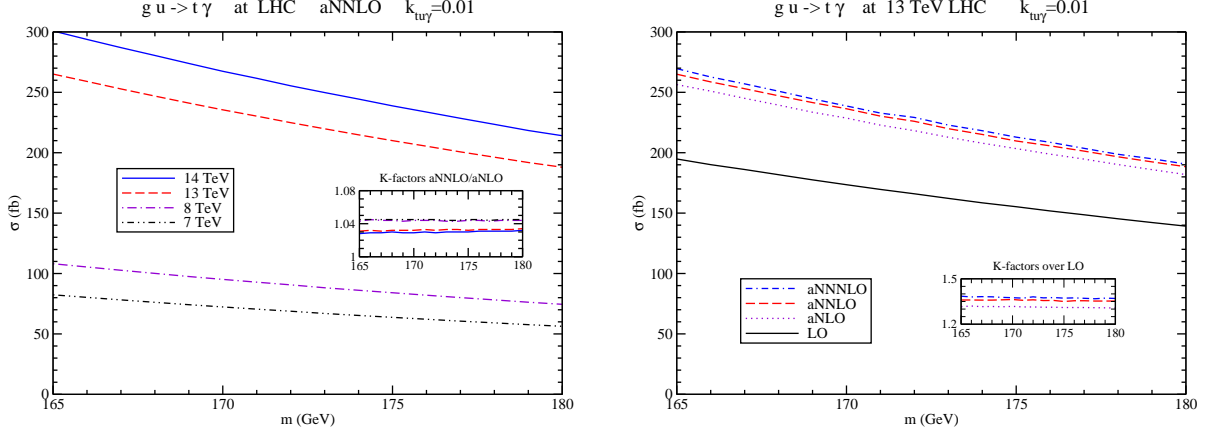


Figure 5: The left plot shows results for the total aNNLO cross section for  $gu \rightarrow t\gamma$  at 7, 8, 13, and 14 TeV as a function of top-quark mass. Its inset shows aNNLO/aNLO  $K$ -factors. The right plot shows the total LO, aNLO, aNNLO, and aNNNLO cross section at 13 TeV as a function of top-quark mass. Its inset shows  $K$ -factors relative to LO.

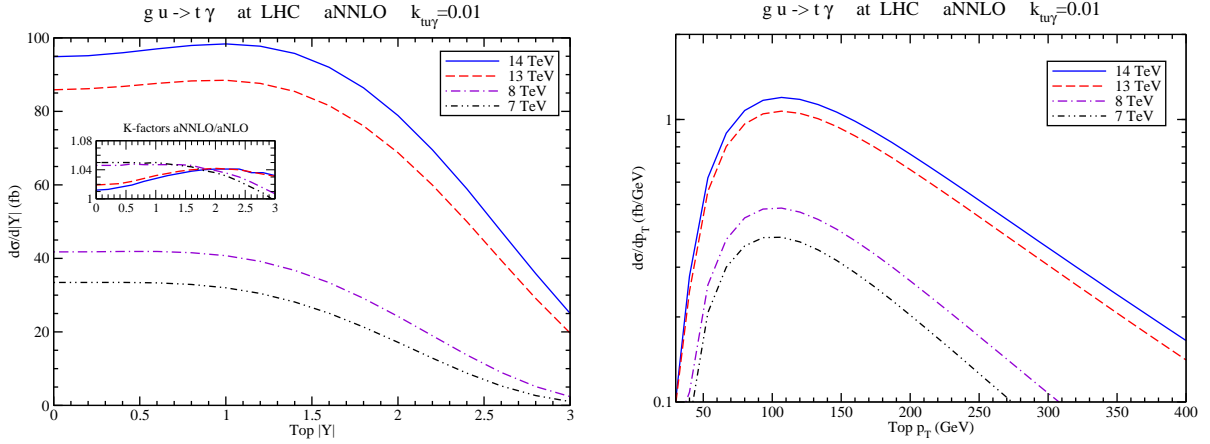


Figure 6: Differential aNNLO rapidity (left plot) and transverse-momentum (right plot) distributions for  $gu \rightarrow t\gamma$  at LHC energies of 7, 8, 13, and 14 TeV. The inset of the rapidity plot also includes  $K$ -factors over aNLO.

## 5 Conclusions

In some physics models beyond the Standard Model, it is possible to have  $tZ$  and  $t\gamma$  production without any additional quarks in the final state. In order to have better experimental limits on these anomalous couplings, we have studied higher-order corrections to both the total cross sections and differential distributions for  $gq \rightarrow tZ$  and  $gq \rightarrow t\gamma$ . These corrections dominate the cross section numerically, and approximate well [14,15] the complete corrections at NLO [6,12]. At aNNLO, they contribute up to a 36% increase at 13 TeV for  $gu \rightarrow t\gamma$  and 49% increase at 13 TeV for  $gu \rightarrow tZ$ . Future work will study soft-gluon corrections in processes with more than two particles in the final state.

## Acknowledgements

This material is based upon work supported by the National Science Foundation under Grant No. PHY 1820795.

## References

- [1] CMS Collaboration, JHEP 04 (2016) 035 [arXiv:1511.03951]
- [2] CMS Collaboration, JHEP 07 (2017) 003 [arXiv:1702.01404]
- [3] ATLAS Collaboration, ATLAS-CONF-2017-070.
- [4] T. Tait and C.-P. Yuan, Phys. Rev. D **63**, 014018 (2000) [hep-ph/0007298].
- [5] N. Kidonakis and A. Belyaev, JHEP **12**, 004 (2003) [hep-ph/0310299].
- [6] Y. Zhang, B.H. Li, C.S. Li, J. Gao, and H.X. Zhu, Phys. Rev. D **83**, 094003 (2011) [arXiv:1101.5346].
- [7] M. Fael and T. Gehrmann, Phys. Rev. D **88**, 033003 (2013) [arXiv:1307.1349].
- [8] J. Adelman *et al.*, arXiv:1309.1947.
- [9] C. Degrande, F. Maltoni, J. Wang, and C. Zhang, Phys. Rev. D **91**, 034024 (2015) [arXiv:1412.5594].
- [10] G. Durieux, F. Maltoni, and C. Zhang, Phys. Rev. D **91**, 074017 (2015) [arXiv:1412.7166].
- [11] Y.-C. Guo, C.-X. Yue, and S. Yang, Eur. Phys. J. C **76**, 596 (2016) [arXiv:1603.00604].
- [12] B.H. Li, Y. Zhang, C.S. Li, J. Gao, and H.X. Zhu, Phys. Rev. D **83**, 114049 (2011) [arXiv:1103.5122].
- [13] J.-L. Agram, J. Andrea, E. Conte, B. Fuks, D. Gele, and P. Lansonneur, Phys. Lett. B **725**, 123 (2013) [arXiv:1304.5551].
- [14] N. Kidonakis, Phys. Rev. D **97**, 034028 (2018) [arXiv:1712.01144]
- [15] M. Forslund and N. Kidonakis, Phys. Rev. D **98**, 074017 (2018) [arXiv:1808.09014].
- [16] N. Kidonakis, Int. J. Mod. Phys. A **33**, 1830021 (2018) [arXiv:1806.03336].
- [17] N. Kidonakis, Phys. Rev. D **99**, 074024 (2019) [arXiv:1901.09928].
- [18] L.A. Harland-Lang, A.D. Martin, P. Molytinski, and R.S. Thorne, Eur. Phys. J. C **75**, 204 (2015) [arXiv:1412.3989].
- [19] S. Dulat, T.-J. Hou, J. Gao, M. Guzzi, J. Huston, P. Nadolsky, J. Pumplin, C. Schmidt, D. Stump, and C.-P. Yuan, Phys. Rev. D **93**, 033006 (2016) [arXiv:1506.07443].